

PAPER • OPEN ACCESS

On the prediction of the time-varying behaviour of dynamic systems by interpolating state-space models

To cite this article: R S O Dias *et al* 2024 *J. Phys.: Conf. Ser.* **2698** 012009

View the [article online](#) for updates and enhancements.

You may also like

- [Effect of shunted piezoelectric control for tuning piezoelectric power harvesting system responses—analytical techniques](#)
M F Lumentut and I M Howard
- [Electromechanical finite element modelling for dynamic analysis of a cantilevered piezoelectric energy harvester with tip mass offset under base excitations](#)
M F Lumentut and I M Howard
- [Influence of temperature on the passive control of a rotating machine using wires of shape memory alloy in the suspension](#)
Marco Túlio Braga, Marco Túlio Santana Alves, Aldemir Ap Cavalini *et al.*

PRIME
PACIFIC RIM MEETING
ON ELECTROCHEMICAL
AND SOLID STATE SCIENCE

HONOLULU, HI
Oct 6–11, 2024

Abstract submission deadline:
April 12, 2024

Learn more and submit!

Joint Meeting of
The Electrochemical Society
•
The Electrochemical Society of Japan
•
Korea Electrochemical Society

On the prediction of the time-varying behaviour of dynamic systems by interpolating state-space models

R S O Dias^{1,*}, M Martarelli¹ and P Chiariotti²

¹ Department of Industrial Engineering and Mathematical Sciences, Università Politecnica delle Marche, 60100 Ancona, Italy

² Department of Mechanical Engineering, Politecnico di Milano, 20156 Milan, Italy

* Corresponding author: R S O Dias, r.dasilva@staff.univpm.it

Abstract. In this article, a local Linear Parameter Varying (LPV) model identification approach is exploited to analyze the dynamic behaviour of a structure whose dynamics varies over time. This structure is composed by two aluminum crosses connected by a rubber mount. To observe time-dependent variations on the dynamics of this assembly, it is placed in a climate chamber and submitted to a six minute temperature run-up. During this run-up the structure is continuously excited by a shaker. The load provided by this device is measured by a load cell, while six accelerometers are measuring the responses of the system. The temperatures of the air inside the climate chamber and at the surface of the mount are also continuously measured. It is found that during the performed temperature run-up, the rubber mount temperature increased from, roughly, 14°C to, approximately, 35.2°C. By using the measured load provided by the shaker and the measured accelerations, Frequency Response Functions (FRFs) at five different rubber mount temperatures are computed. From each of these sets of FRFs, state-space models are estimated. Afterwards, these models are used to define an interpolating LPV model, which enables the computation of interpolated state-space models representative of the dynamics of the system at each time sample. It is found that by feeding the interpolated state-space models with the measured load, an accurate simulation of the measured accelerations is obtained. Moreover, by exploiting a joint input-state estimation algorithm with the interpolated state-space models and with the measured accelerations, a very good prediction of the applied load can be obtained. It is also shown that if the time dependency of the dynamics of the system is ignored, the results are less accurate.

Keywords: Structural Dynamic Measurements, Linear Parameter Varying models, System Identification, Load Identification, Joint input-state estimation, State-Space Models

1. Introduction

Nowadays, the characterization of the dynamic behaviour of components presenting time-varying performances is gaining attention. This is due to the fact that many mechanical systems are composed by parts, whose dynamics can significantly change over time when these mechanical systems are running under normal operating conditions. A classical example of these parts are the rubber mounts (which are commonly used in the automotive industry [1]), whose dynamic stiffness is highly dependent on many factors, for instance, on temperature and on the applied static pre-load (see [2], [3], [4]). To analyze the dynamic behaviour of components presenting time-varying mechanical behaviour, the use of time domain approaches is advantageous, because, by working on this domain, we can analyze components presenting time-domain variations on their dynamics and submitted to any kind of excitation.



An interesting way of representing the dynamics of a given system in time-domain is by exploiting the state-space formulation. This formulation is suited to deal with time-domain formulated problems and it is one of the best choices to tackle real-time applications. Furthermore, the state-space formulation can be used to characterize the dynamics of components presenting time-varying dynamic behaviour. This can be done by exploiting the so-called Linear Parameter Varying models (LPV), which find applications on different areas [5], for instance, on automotive (see, for example [6]) and mechatronics (see, for instance, [7]). The approaches used to identify LPV models are, in general, clustered in two groups: the group of the global approaches and the group of the local approaches [8]. The global approaches enable the computation of the LPV model by testing the system under study, while its dynamics is continuously changing over time (see, for example, [9]). Conversely, by following the local approaches, a set of Linear Time-Invariant (LTI) state-space models representative of the dynamics of the system for fixed operating conditions is interpolated to obtain state-space models representative of the system for intermediate operating conditions. This interpolation is performed by exploiting an interpolating LPV model computed from the estimated set of LTI models (e.g. approaches presented in [10], [11]). Here, a local approach will be exploited.

The use of LPV models is indeed advantageous as it enables the characterization of assembled systems presenting time-varying dynamic behaviour subjected to any kind of excitation. In alternative, one may also think on exploiting these LPV models to characterize the dynamic behaviour of simple components presenting time-varying dynamic behaviour, which can then be included in the complete assembly through State-Space Substructuring (see, for instance, [12], [13], [14], [15]).

The present article aims at demonstrating the need of taking into account possible time-domain variations on the dynamics of real mechanical systems in order to perform accurate predictions of their time-domain responses and of the time-domain loads applied on them. Furthermore, we also aim at demonstrating the accuracy and the reliability of the interpolating LPV models constructed from a set of state-space models identified from measured FRFs to tackle vibro-acoustic applications involving the characterization of real systems presenting time-varying dynamic behaviour.

The methodology exploited to compute LPV models is presented in section 2, whereas in section 3 this methodology is validated on an experimental scenario. Finally, the conclusions of this paper are presented in section 4.

2. Construction of Linear Parameter Varying models

The methodology used in this article to compute LPV models will be here presented in short. This methodology belongs to the group of the local approaches (see section 1) and involves three different steps. Firstly, state-space models representative of the dynamics of the system under analyze for specific pre-selected fixed operating conditions are identified. Secondly, each of these state-space models must be transformed into the same coherent representation. Thirdly, an interpolating LPV model is constructed from the set of coherent state-space models obtained from the second step. Note that, through this section we will assume that the LPV model will be set-up from LTI displacement state-space models. In this way, as discussed in [16], we are able to reduce the amount of variables involved in the computation of the LPV model. Thereby, leading to the reduction of the computational cost associated with the computation of the LPV model and with the computation of interpolated state-space models representative of the dynamics of the system for each of the intermediate operational conditions. Furthermore, we will assume that the fixed operating conditions associated with each of the LTI state-space models are characterized by a single scheduling parameter (for example, by the temperature at which the system is submitted).

To select the fixed operating conditions for which state-space models will be estimated, we

must identify the maximum and minimum values of interest for the scheduling parameter (i.e. $\bar{\beta}$ and $\underline{\beta}$, respectively) that is responsible for changing the dynamics of the system under study (for example, the maximum and minimum temperatures to which the system is submitted). Then, one must select a set of fixed operating conditions characterized by different values of the scheduling parameter, for which state-space models will be identified. No strict rules exist to define the number of state-space models that must be identified, neither to select the values of the scheduling parameter associated with each of them. Nevertheless, few guidelines can be here mentioned. To avoid extrapolation, one must select at least one fixed operating condition characterized by a value of the scheduling parameter that is equal or higher than $\bar{\beta}$, and one fixed operating condition characterized by a value of the scheduling parameter that is equal or lower than $\underline{\beta}$. It is also suggested that the set of selected operating conditions must make sure that the LTI models are characterized by equidistant values of the scheduling parameter. Furthermore, the selected fixed operating conditions must ensure that no abrupt variations on the dynamics of the mechanical system are observed between consecutive fixed operating conditions in order to enable a smooth interpolation of the LTI models (see [7]).

After selecting the fixed operating conditions to be used to set-up the LPV model, LTI state-space models representative of those conditions must be identified. However, if the set of state-space models is estimated from data acquired experimentally (which is the strategy that we will follow in this paper), such a set is generally not identified in a coherent representation [16]. Hence, the identified models cannot be directly used to set-up an LPV model (see, for example, [8],[7]). To coherently represent each of the estimated state-space models, we will follow the procedure discussed in [16]. By following this approach, we must make sure that all the identified models are represented in complex diagonal form (see [17]). Then, the poles of each model must be coherently sorted. This can be done by sorting the poles in terms of ascending damped natural frequency. To break ties when sorting pairs of complex conjugate poles, we may, for example, include firstly the pole presenting positive imaginary part. Note that, when sorting each pole, we must sort accordingly the associated row of the input matrix and the associated column of the output matrix [16]. To finally obtain a coherent representation of the set of identified state-space models, the input and output matrices of each of these models must be coherently scaled. A possible approach to perform this scaling is to normalize each row of the input matrix with respect to one of its columns (see [18],[16]).

As next step, a LPV model must be set-up by using the computed coherent set of identified models. To construct the LPV model, we will follow the strategy proposed in [7]. When exploiting this approach, we assume that the LPV model to be constructed presents an homogeneous polynomial dependency on the values that the parameterization of the scheduling parameter takes in a multisimplex Λ . To implement this approach, we must start by selecting the dimension of the multisimplex Λ in order to parameterize a given scheduling parameter β . A common choice for the dimension of the multisimplex Λ is $N = 2$, hence, we can parameterize the value of β associated with a given fixed operating condition i as given hereafter.

$$\alpha_{\beta,1} = \frac{\beta_i - \underline{\beta}}{\bar{\beta} - \underline{\beta}}, \quad \alpha_{\beta,2} = 1 - \alpha_{\beta,1} \quad (1)$$

At this moment, we can define the state-space matrices of the interpolated state-space model representative of the fixed operating condition i computed from the LPV model to be set-up as follows:

$$\text{diag}[A(\alpha_i)] = \sum_{k=1}^{J_N(g)} \alpha_i^k \{\tilde{A}^k\} \quad (2a)$$

$$[B(\alpha_i)] = \sum_{k=1}^{J_N(g)} \alpha_i^k [\tilde{B}^k] \quad (2b)$$

$$[C(\alpha_i)] = \sum_{k=1}^{J_N(g)} \alpha_i^k [\tilde{C}^k] \quad (2c)$$

where, $\text{diag}[\bullet]$ is a column vector containing the diagonal elements of matrix $[\bullet]$, while α_i^k represents the element located on the k^{th} column of $\{\alpha_i\}$, which is given below.

$$\{\alpha_i\} = \begin{bmatrix} \alpha_{\beta,1}^g \alpha_{\beta,2}^0 & \alpha_{\beta,1}^{g-1} \alpha_{\beta,2}^1 & \dots & \alpha_{\beta,1}^0 \alpha_{\beta,2}^g \end{bmatrix} \quad (3)$$

Note that, all the elements of $\{\alpha_i\}$ present the same degree, because the approach proposed in [7] assumes that the LPV model presents an homogeneous polynomial dependency on the values that the parameterization of the scheduling parameter takes in a multisimplex Λ (see equation (1)). The number of columns of $\{\alpha_i\}$ can be calculated by using the expression given below.

$$J_N(g) = \frac{(N+g-1)!}{g!(N-1)!} \quad (4)$$

To set-up the interpolating LPV model, the variables $\{\tilde{A}^k\} \in \mathbb{C}^{n \times 1}$, $[\tilde{B}^k] \in \mathbb{C}^{n \times n_i}$ and $[\tilde{C}^k] \in \mathbb{C}^{n_o \times n}$ present in expression (2) must be calculated. To determine these variables, we will formulate our problem as follows:

$$[a]\{q\} = \{b\} \quad (5)$$

where,

$$[a] = \begin{bmatrix} \alpha_1 \otimes I_{A,A} \\ \vdots \\ \alpha_m \otimes I_{A,A} & \alpha_1 \otimes I_{B,B} \\ & \vdots \\ & \alpha_m \otimes I_{B,B} & \alpha_1 \otimes I_{C,C} \\ & & \vdots \\ & & \alpha_m \otimes I_{C,C} \end{bmatrix} \quad (6a)$$

$$\{q\} = \{\{q_A\}^T \quad \{q_B\}^T \quad \{q_C\}^T\}^T \quad (6b)$$

$$\{b\} = \{\{b_A\}^T \quad \{b_B\}^T \quad \{b_C\}^T\}^T \quad (6c)$$

with,

$$\begin{aligned}
\{q_A\} &= \{\{\tilde{A}^1\}^T \quad \dots \quad \{\tilde{A}^{J_N(g)}\}^T\}^T \\
\{q_B\} &= \{(vec[\tilde{B}^1])^T \quad \dots \quad (vec[\tilde{B}^{J_N(g)}])^T\}^T \\
\{q_C\} &= \{(vec[\tilde{C}^1])^T \quad \dots \quad (vec[\tilde{C}^{J_N(g)}])^T\}^T \\
\{b_A\} &= \{(diag[A_{cdf}^1])^T \quad \dots \quad (diag[A_{cdf}^m])^T\}^T \\
\{b_B\} &= \{(vec[B_{cdf,sc}^1])^T \quad \dots \quad (vec[B_{cdf,sc}^m])^T\}^T \\
\{b_C\} &= \{(vec[C_{cdf,sc}^1])^T \quad \dots \quad (vec[C_{cdf,sc}^m])^T\}^T
\end{aligned} \tag{7}$$

where, $[I_{A,A}] \in R^{n \times n}$, $[I_{B,B}] \in R^{(n \times n_i) \times (n \times n_i)}$ and $[I_{C,C}] \in R^{(n \times n_o) \times (n \times n_o)}$ are identity matrices, $vec[\bullet]$ is the vector obtained by stacking all columns of matrix $[\bullet]$, \otimes denotes the Kronecker matrix product (see, for example, [19]), while m is the number of models used to construct the LPV model. Subscript *cdf* denotes state-space matrices belonging to a model transformed into complex diagonal form (see [17]), whereas subscript *sc* denotes input and output state-space matrices that were coherently scaled. To determine the value of the unknown variables included in $\{q\}$, we can simply determine this vector in a linear least-squares sense as follows:

$$\{q\} = [a]^\dagger \{b\} \tag{8}$$

the error vector associated with the calculation of $\{q\}$ can be determined as given below.

$$\{E(q)\} = \begin{bmatrix} diag[A_{cdf}^1] - \sum_{k=1}^{J_N(g)} \alpha_1^k \{\tilde{A}^k\} \\ \vdots \\ diag[A_{cdf}^m] - \sum_{k=1}^{J_N(g)} \alpha_m^k \{\tilde{A}^k\} \\ vec[B_{cdf,sc}^1] - \sum_{k=1}^{J_N(g)} \alpha_1^k vec[\tilde{B}^k] \\ \vdots \\ vec[B_{cdf,sc}^m] - \sum_{k=1}^{J_N(g)} \alpha_m^k vec[\tilde{B}^k] \\ vec[C_{cdf,sc}^1] - \sum_{k=1}^{J_N(g)} \alpha_1^k vec[\tilde{C}^k] \\ \vdots \\ vec[C_{cdf,sc}^m] - \sum_{k=1}^{J_N(g)} \alpha_m^k vec[\tilde{C}^k] \end{bmatrix} \tag{9}$$

Note that, the number of variables to be computed with the used linear least-squares formulation (see expression (5)) to set-up the LPV model can be halved, in case that the estimated state-space models are only composed by pairs of complex conjugate poles (for example, if these models are computed by following the methodology proposed in [20]). Thus, the number of variables to be computed to calculate interpolated state-space models by exploiting the computed LPV models can be halved as well.

3. Experimental validation

3.1. Testing Campaign

In this section, the methodology presented in section 2 will be exploited to construct a LPV model representative of the dynamic behaviour of a structure whose dynamics is time-dependent. This structure is composed by two aluminum crosses connected by a rubber mount (see figure 1).

To observe time-dependent variations on the dynamics of this assembly, the assembled system was placed in a climate chamber and heated during a six minute temperature run-up. In this

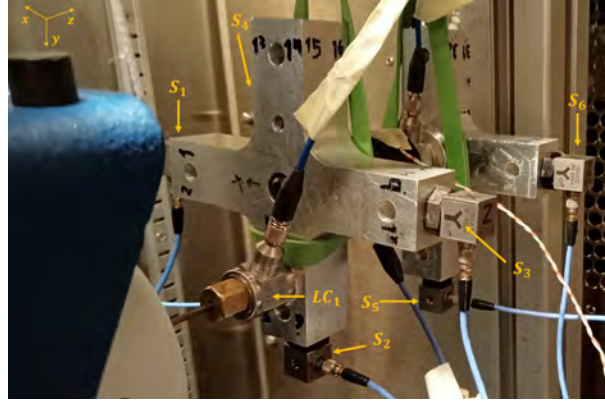


Figure 1. Test set-up used to experimentally characterize the assembly under study.

way, the mechanical behaviour of the rubber mount changed over time leading to a time-domain variation of the mechanical behaviour of the complete assembly. During the run-up the structure was continuously excited by a shaker. To control the excitation provided by the shaker and the band of excited frequencies, this device was fed with a random signal constructed as

$$v(t_k) = \sum_{f=10}^{250} \gamma_{f,k} \cos(2 \times 2\pi f + \phi_{f,k}) \quad (10)$$

where, $\gamma_{f,k}$ and $\phi_{f,k}$ are Gaussian distributed stochastic variables, whose means are 5×10^{-2} V and 0 rad, respectively. The standard deviation of variables $\gamma_{f,k}$ and $\phi_{f,k}$ is 1×10^{-2} V and 2 rad, respectively.

Note that, the aim of the present article is to show the importance of taking into account possible time-domain variations on the dynamics of real mechanical systems and to demonstrate the accuracy of the LPV models computed by following the methodology presented in section 2 to characterize the dynamical behaviour of this kind of systems. Hence, any kind of signal that excites frequencies included in the frequency band for which the dynamics of the system is relevant (i.e. approximately, from 20 Hz to 500 Hz (see [14],[15])) could have been used.

During the performed temperature run-up, the load provided by the shaker was measured by a load cell, while three accelerometers were placed on both the aluminum crosses to measure the responses of the system (see figure 1). The air temperature inside the climate chamber and the temperature at the surface of the mount were also continuously measured by using two different thermocouples (type T). The registered temperatures during the run-up are shown in figure 2.

3.2. Computation of the Linear Parameter Varying model

In this section, an LPV model representative of the dynamics of the system under study will be constructed. To construct this model, we must start by estimating a set of LTI state-space models representative of the dynamics of the system for some selected fixed operating conditions. By observing figure 2 we see that the temperature at the surface of the rubber mount (from now on tagged as T_{rb}) ranges, roughly, from a minimum value of 14°C to a maximum value of, approximately, 35.2°C. Hence, to avoid extrapolation, two of the state-space models to be used on the construction of the LPV model must be representative of the dynamics of the system for $T_{rb} = 14^\circ\text{C}$ and $T_{rb} = 35.2^\circ\text{C}$. To make sure that the set of computed state-space models well captures the dynamic behaviour of the structure between $T_{rb} = 14^\circ\text{C}$ and $T_{rb} = 35.2^\circ\text{C}$ and that the variation on the dynamics of the system is smooth between consecutive fixed operating conditions, we have decided to estimate three additional state-space models representative of the

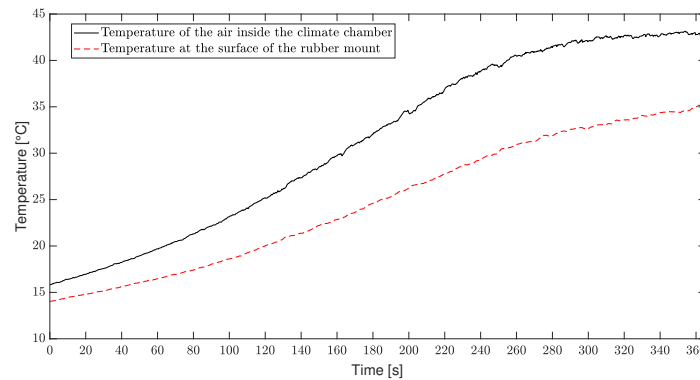


Figure 2. Temperatures of the air inside the climate chamber and at the surface of the rubber mount registered during the performed experimental test.

dynamics of the assembly associated with rubber mount temperatures of 20°C, 25°C and 30°C. To compute these state-space models, we must start by computing the FRFs of the system for the rubber mount temperatures of interest (i.e. 14°C, 20°C, 25°C, 30°C and 35.2°C). In addition, to have the possibility of validating the LPV model to be constructed, we will also compute the FRFs of the system for $T_{rb} = 27.5^\circ\text{C}$, which is a temperature in between the rubber mount temperatures associated with the models that will be identified. To compute the intended FRFs, chunks of the time-domain acceleration signals measured with the accelerometers and of the time-domain load signal measured by the load cell will be used. The initial time instant of the chunks of both accelerations and load signals used to compute each set of FRFs will be defined by searching on the curve of the registered temperatures at the surface of the rubber mount (see figure 2) for the instant at which the temperature of the mount is the temperature associated with the set of FRFs to be computed minus, roughly, 0.5°C. Similarly, to define the final instants of the chunks of signals used to determine each set of FRFs, we must search on the curve of the registered temperatures at the surface of the rubber mount (see figure 2) for the instant at which the temperature of the mount is the temperature associated with the set of FRFs to be computed plus, approximately, 0.5°C. In table 1 are shown the selected initial and final time instants to extract the chunks of signals used to compute each set of FRFs (associated with rubber mount temperatures of 14°C, 20°C, 25°C, 27.5°C, 30°C and 35.2°C) and the temperatures measured at the surface of the rubber mount at those time instants.

Table 1. Selected initial and final time instants to define the chunks of signals used to compute each set of FRFs and temperatures measured at the surface of the mount at those time instants.

T_{rb} (°C)	$t_{initial}$ (s)	t_{final} (s)	$T_{initial}$ (°C)	T_{final} (°C)
14	11	38	14.5	15.5
20	113.5	127	19.5	20.5
25	178.5	192	24.5	25.5
27.5	211	223	27	28
30	241.5	252.5	29.5	30.5
35.2	352	361	34.5	35.2

It is worth mentioning that, the chunks of signals were selected as described above to enable

the possibility of computing several averages of each set of FRFs. Note also that, to compute the set of FRFs for $T_{rb} = 14^\circ\text{C}$, we decided to select the initial time instant of the chunks of signals to be associated with a rubber mount temperature of 14.5°C (see table 1). This choice is justified by the fact that at beginning of the test, the structure was in steady-state. Hence, to make sure that since the beginning of the selected chunks of signals, the structure was being well excited, we decided to select the initial time instant of the chunks of signals to be associated with an higher rubber mount temperature (which leads to the selection of an higher initial time instant). Moreover, it is not expected that the FRFs change significantly due to a 0.5°C difference on the temperature of the mount. Thus, the defined chunks of signal will, in principal, lead to an accurate computation of the FRFs of the system for $T_{rb} = 14^\circ\text{C}$.

By using the chunks of signal defined in table 1, the sets of FRFs representative of the dynamic behaviour of the component under study for rubber mount temperatures of 14°C , 20°C , 25°C , 27.5°C , 30°C and 35.2°C were calculated. It is worth mentioning that to enable the calculation of more averages, an overlap process with 50% of overlap was exploited. Moreover, to minimize the effect of leakage on the calculated sets of FRFs, an Hanning window was applied on both output and input time-signals used to calculate each average of each set of FRFs (see [21]). In figure 3, it is shown the comparison of the calculated FRFs, whose output is S_4^y (where, the superscript refers to the direction of the output) and the input is LC_1^z (where, the superscript refers to the direction of the input) (see figure 1), of the structure under analyze for the rubber mount temperatures associated with the state-space models to be identified, i.e. 14°C , 20°C , 25°C , 30°C and 35.2°C .

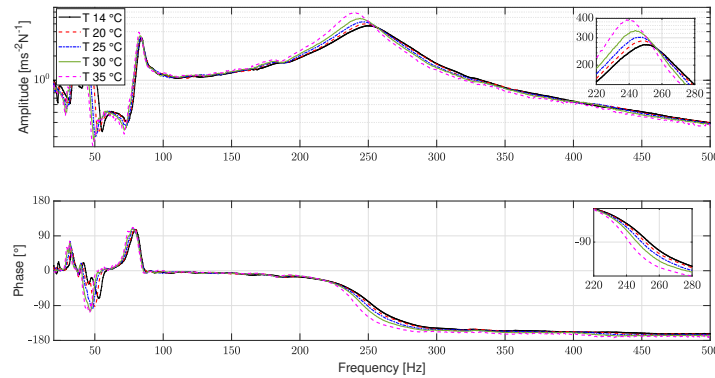


Figure 3. Comparison of the calculated FRFs, whose output is S_4^y and the input is LC_1^z , of the structure under study for the following rubber mount temperatures: 14°C , 20°C , 25°C , 30°C and 35.2°C .

By observing figure 3, it is evident that the FRFs of the system change with the rubber mount temperature, specially for frequencies between 200 Hz and 300 Hz. It is also evident that as the rubber mount temperature increases, the resonance of the FRFs located between 200 Hz and 300 Hz is shifted towards lower frequencies and its amplitude increases. This is, indeed, expected, because it is well-know that the dynamic stiffness of rubber mounts decreases as the temperature at which they are submitted increases (see [22],[23]). Furthermore, it can be observed that the variation of the FRF between consecutive selected fixed operating conditions is smooth. Thus, the chosen fixed operating conditions are in principle good choices for the computation of an interpolating LPV model (see section 2).

At this point, state-space models must be estimated from the computed sets of FRFs (from now on tagged as measured sets of FRFs) representative of the dynamics of the system for rubber

mount temperatures of 14°C, 20°C, 25°C, 30°C and 35.2°C. To estimate those models, we started by exploiting the Simcenter Testlab[®] implementation of both PolyMAX (see, [24]) and ML-MM (see, [25]) methods to obtain reliable modal parameters representative of the set of measured FRFs associated with $T_{rb} = 14^\circ\text{C}$. Then, to obtain the modal parameters representative of the dynamics of the assembly for the other rubber mount temperatures of interest, we have exploited the ML-MM method to update the modal parameters estimated from the measured FRFs for $T_{rb} = 14^\circ\text{C}$. Afterwards, by following the procedures described in [20],[26], state-space models representative of the dynamics of the system for rubber mount temperatures of 14°C, 20°C, 25°C, 30°C and 35.2°C were constructed by using the estimated modal parameters.

Note that, the modal parameters were estimated by assuming a proportionally damped model. By performing this assumption, we have the guarantee that the residue matrices of the computed modal models will be purely imaginary. In this way, we make sure that the state-space models will obey Newton's second law (see [26]). If the modal parameters used to construct the state-space models have not been computed by assuming a proportionally damped modal model, we would be required to force them to verify Newton's second law by following the approach proposed in [27]. However, this approach makes use of undamped residual compensation modes (RCMs). As we intend to use the estimated state-space models to construct a LPV model to perform time-domain simulations, it is not recommended to include undamped modes on the estimated models, because they can give rise to numerical instabilities [20].

It is also worth mentioning, that each of the computed state-space models is composed by 14 states. Each of these models includes 5 in-band pairs of complex conjugate poles, 2 RCMs responsible for including the contribution of the lower out-of-band modes in the frequency band of interest and 2 additional RCMs that model the contribution of the upper out-of-band modes in the frequency band of interest. The RCMs responsible for including the contribution of the lower out-of-band modes were set-up by selecting a value for their natural frequencies and damping ratios of 0.1 Hz and 0.1, respectively. Whereas, the RCMs responsible for including the contribution of the upper out-of-band modes were set-up by selecting a value for their natural frequencies and damping ratios of 1.5×10^3 Hz and 0.1, respectively (see, [20],[26]).

Figure 4 shows the comparison of the measured accelerance FRF, whose output is S_6^z and the input is LC_1^z , of the assembly at 30°C with the same accelerance FRF of the correspondent estimated state-space model.

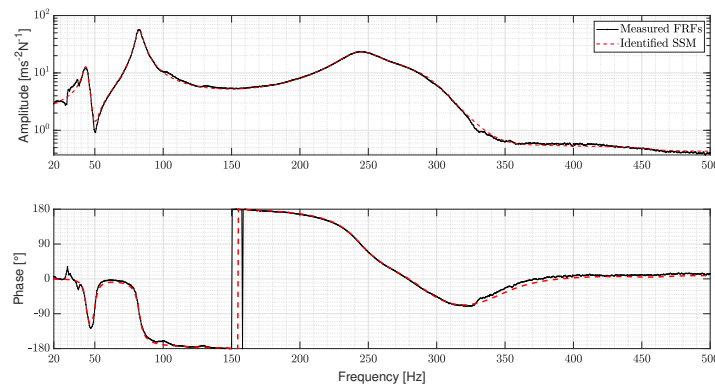


Figure 4. Comparison of the measured accelerance FRF, whose output is S_7^z and the input is LC_1^z , of the assembly for $T_{rb} = 30^\circ\text{C}$ with the same accelerance FRF of the correspondent identified state-space model.

By observing figure 4, it is evident that both FRFs are well-matching, hence we may conclude

that the estimated state-space model is reliable to characterize the dynamics of the system for $T_{rb} = 30^\circ\text{C}$. A similar match quality was observed between the measured FRFs associated with the other rubber mount temperatures of interest and the FRFs of the correspondent identified state-space models.

After having identified the intended set of state-space models, we must transform these models into a coherent representation by following the procedures presented in section 2. Then, by using the obtained set of coherent models, the LPV model can finally be constructed. However, to compute the LPV model, we must firstly define the degree g of the homogeneous polynomial dependency of the LPV model on the parameterized values of the rubber mount temperatures associated with each of the identified state-space models (which is the scheduling parameter that characterizes the dynamics of the assembly under study) (see section 2). Unfortunately, there is no knowledge regarding the dependency of the dynamics of the system under study on the rubber mount temperature. Hence, to select a degree of dependency that leads to the computation of an accurate LPV model, we computed several LPV models by selecting different values for g ranging from 1 to 4. For each of the computed LPV models, the 2-norm error associated with the solved linear-least squares problems to define each of them was computed. These 2-norm errors are reported in table 2.

Table 2. 2-norm errors of the solved linear-least squares problems to set-up LPV models by assuming values of g ranging from 1 to 4.

g	1	2	3	4
$\ E(q)\ $	54.0184	12.3166	8.2350	2.7847×10^{-11}

By analyzing table 2, we conclude that the value of the 2-norm error associated with the computation of the LPV model by assuming $g = 4$ is very close to zero. This means that the LPV model associated with $g = 4$ enables the construction of state-space models for the rubber mount temperatures associated with the set of identified models, whose state-space matrices elements are almost equal to the elements of the state-space matrices of the correspondent identified models. Hence, assuming that the influence of T_{rb} over the dynamics of the system under analysis can be accurately captured by the set of identified models, it is very likely that the constructed LPV model by assuming $g = 4$ properly models the dependency of the dynamics of the assembly under study on the rubber mount temperature. Therefore, we expect the computed interpolated models representative of the system for rubber mount temperatures in between the temperatures associated with the identified models to be accurate and reliable. If this is the case, the variation of the FRFs of the interpolated state-space models computed by the defined LPV model must be smooth for values of T_{rb} ranging from 14°C to 35.2°C (see figure 3). In figure 5, it is shown a surface defined from the accelerance FRF, whose output is S_4^y and the input is LC_1^z , of the interpolated state-space models representative of the dynamics of the system for rubber mount temperatures spaced by 0.1°C and ranging from 14°C to 35.2°C .

By observing figure 5, it is evident that the FRF of the interpolated state-space models shown in this figure presents a smooth variation with the rubber mount temperature. The same smooth variation is observed for the other FRFs of the interpolated state-space models. Hence, this suggests that the LPV model was properly computed and that it is reliable to compute interpolated state-space models for values of T_{rb} ranging from 14°C to 35.2°C .

Nevertheless, to make sure that the computed LPV model is, in fact, accurate, we will compare the FRFs of the interpolated state-space model representative of the dynamics of the system for $T_{rb} = 27.5^\circ\text{C}$ with the correspondent measured FRFs. In figure 6, the mentioned comparison is performed for the accelerance FRF, whose output is S_2^z and the input is LC_1^z .

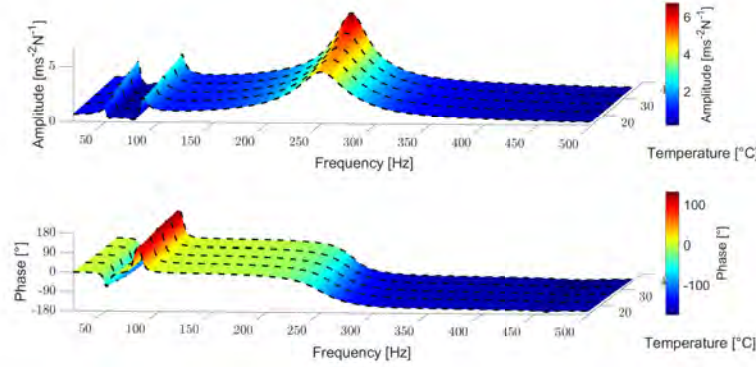


Figure 5. Surface defined from the accelerance FRF, whose output is S_4^y and the input is LC_1^z , of the interpolated state-space models representative of the dynamics of the system for rubber mount temperatures spaced by 0.1°C and ranging from 14°C to 35.2°C .

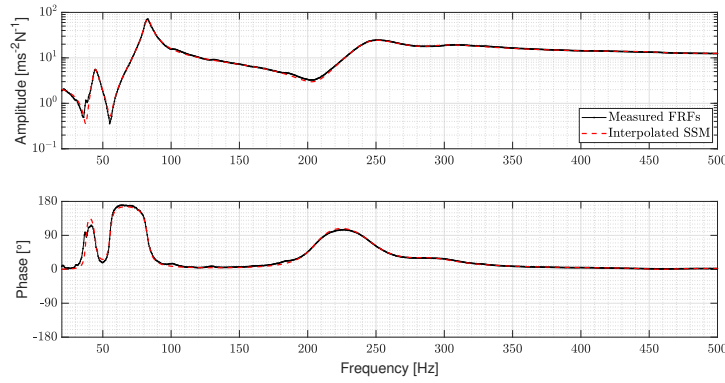


Figure 6. Comparison of the measured accelerance FRF, whose output is S_2^z and the input is LC_1^z , of the assembly for $T_{rb} = 27.5^\circ\text{C}$ with the same accelerance FRF of the correspondent interpolated state-space model computed by using the LPV model defined by assuming $g = 4$.

By observing figure 6, it is evident that the FRF of the interpolated state-space model very well-matches the correspondent measured FRF. This observation further proves that the LPV model defined by assuming $g = 4$ is indeed accurate to compute state-space models that well represent the dynamics of the system for values of T_{rb} ranging from 14°C to 35.2°C .

3.3. Time-domain responses simulation and time-domain load identification

In this section, we will start by reconstructing the time-domain responses acquired during the performed experimental test (see section 3.1) by using the measured time-domain load signal and the interpolated state-space models generated by the LPV model computed in section 3.2. Furthermore, to evaluate the importance of taking into account the time-domain variation of the dynamics of the system under study, the same reconstruction will be performed by using the identified LTI state-space model representative of the dynamics of the system for $T_{rb} = 14^\circ\text{C}$.

Figures 7 and 8 show the comparison of the measured time-domain response of two different outputs with the simulated responses of the same outputs computed i) by using the state-space model representative of the dynamics of the assembly for $T_{rb} = 14^\circ\text{C}$ and ii) by using the interpolated state-space models obtained at each time sample with the computed LPV model.

It is worth mentioning that to focus our analysis on frequencies for which the variation of the rubber mount temperature has an important influence over the FRFs of the system under analyze (see figure 3), we have re-constructed the measured time-domain acceleration signals by using the measured time-domain load signal filtered with a band-pass filter, whose pass-band frequencies range from 120 Hz to 350 Hz.

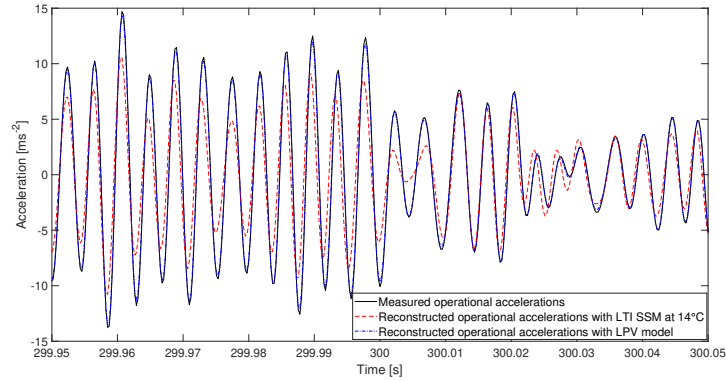


Figure 7. Comparison of the measured time-domain response of output S_7^z with the simulated response of the same output computed i) by using the state-space model representative of the dynamics of the assembly for $T_{rb} = 14^\circ\text{C}$ and ii) by using the interpolated state-space models obtained at each time sample with the computed LPV model.

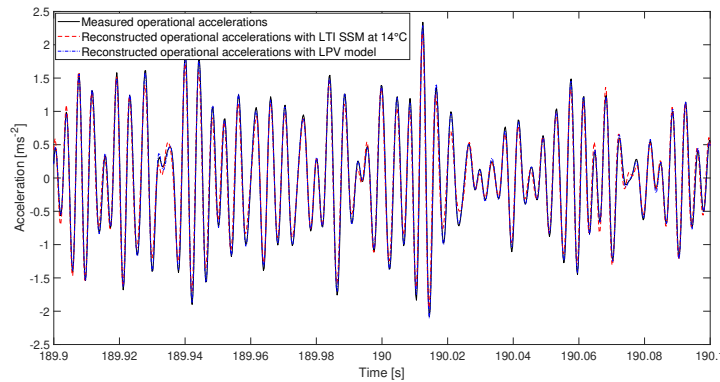


Figure 8. Comparison of the measured time-domain response of output S_8^y with the simulated response of the same output computed i) by using the state-space model representative of the dynamics of the assembly for $T_{rb} = 14^\circ\text{C}$ and ii) by using the interpolated state-space models obtained at each time sample with the computed LPV model.

By observing figures 7 and 8, it is evident that the simulated time-domain responses by using the interpolated models are very well-matching the correspondent measured time-domain responses. In contrast, the time-domain responses computed by the state-space model representative of the dynamics of the system for $T_{rb} = 14^\circ\text{C}$ are not matching the measured time-domain responses so closely. As expected, this is specially true for time intervals corresponding to higher values of T_{rb} (see figures 7 and 8). Hence, we may conclude that the procedures presented in section 2 are valid to compute interpolating LPV models that accurately characterize the

dynamic behaviour of real mechanical systems presenting important time-domain variations on their dynamics. Moreover, this comparison shows the importance of taking into account possible time-domain variations on the dynamics of mechanical systems in order to perform reliable time-domain simulations.

As final analysis, the time-domain responses measured during the performed experimental test (see section 3.1) will be used with the joint input-state estimation algorithm proposed in [28] to estimate the time-domain load applied by the shaker. In figure 9, it is shown the comparison of the measured time-domain load with the time-domain loads estimated by using the joint input-state estimator algorithm and the measured time-domain responses with a) the state-space model of the system under analyze for $T_{rb} = 14^\circ\text{C}$ and with b) the interpolated state-space models estimated at each time sample by exploiting the computed LPV model.

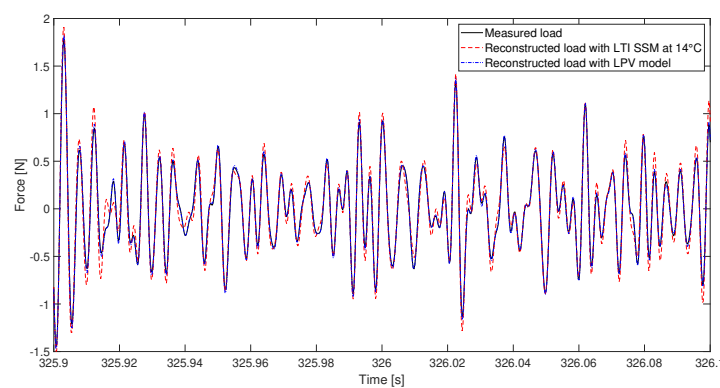


Figure 9. Comparison of the measured time-domain load with the time-domain loads estimated by using the joint input-state estimator algorithm and the measured time-domain responses with a) the state-space model of the system under analyze for $T_{rb} = 14^\circ\text{C}$ and with b) the interpolated state-space models estimated at each time sample by exploiting the computed LPV model.

By observing figure 9, we can conclude that the time-domain load estimated with the interpolated state-space models is very well-matching the time-domain load measured by the load cell. Furthermore, it is evident that the use of the state-space model representative of the system for $T_{rb} = 14^\circ\text{C}$ to estimate the applied time-domain load leads to less accurate results. Hence, this comparison demonstrates that to perform accurate time-domain load identifications, we must take into account possible time-domain variations on the dynamics of the components under analysis.

Note that, as the x direction of the system under study is not well excited by the shaker (see figure 1), the time-domain acceleration signals measured in this direction were not used to reconstruct the measured time-domain load signal. Moreover, to focus our analysis on frequencies for which the variation of the rubber mount temperature has an important influence over the FRFs of the system (see figure 3), we have re-constructed the measured time-domain load signal by using the measured time-domain acceleration signals filtered with a band-pass filter, whose pass-band frequencies range from 120 Hz to 350 Hz.

It is also worth mentioning that to initialize the joint input-state estimation algorithm, we are required to define the state vector at the initial time instant and the associated covariance matrix. In addition, we are also required to provide the covariance matrices associated with the process noise and with the measurement noise (see [28]). The initial state vector and the associated covariance matrix were defined to be null, because at the beginning of the performed experimental test, the system was in steady-state. As the estimated state-space models are

accurate and reliable (see figures 4 and 6), the covariance matrix associated with the process noise was assumed to be null, whereas the covariance matrix associated with the measurement noise was calculated from the statistical noise properties of the accelerometers provided by the manufacture (see [29]). Furthermore, we have assumed that the measurement noise of the different accelerometers is uncorrelated with each other. Thereby, this covariance matrix was defined to be $6.16 \times 10^{-6} \times [I]$, where $[I]$ is a unitary matrix of dimension $n_l \times n_l$ (with n_l representing the number of outputs used to reconstruct the load applied on the system).

4. Conclusion

The use of an interpolating LPV model computed by following the procedures presented in section 2, revealed to be an accurate approach to characterize the time-varying dynamical behaviour of an assembly composed by two aluminum crosses connected by a rubber mount submitted to a temperature run-up. In addition, it was shown that by using interpolated state-space models representative of the mechanical behaviour of this system at each time sample, reliable estimations of its time-domain responses could be obtained. The same was shown to be valid for the estimation of the applied time-domain load. Moreover, it was evident that if the time-domain variation of the dynamics of the system is ignored, the accuracy of the predicted time-domain responses and load is deteriorated. Hence, this study opens perspectives to use interpolating LPV models defined by following the methodology discussed in section 2 to characterize mechanical systems with higher complexity or to characterize simple components presenting time-varying dynamic behaviour, which can then be included in the complete assembly through State-Space Substructuring.

Funding

This project has received funding from the European Union's Framework Programme for Research and Innovation Horizon 2020 (2014-2020) under the Marie Skłodowska-Curie Grant Agreement n° 858018.

References

- [1] A.E. Mahmoudi, D.J. Rixen, and C.H. Meyer. Comparison of Different Approaches to Include Connection Elements into Frequency-Based Substructuring. *Experimental Techniques*, 2020.
- [2] C.A.J. Beijers and A. de Boer. Numerical modelling of rubber vibration isolators. In *Tenth International Conference on Sound and Vibration*, Stockholm, Sweden, 2003.
- [3] T. Roncen, J.-J. Sinou, and J.-P. Lambelin. Experiments and nonlinear simulations of a rubber isolator subjected to harmonic and random vibrations. *Journal of Sound and Vibration*, 451:71–83, 2019.
- [4] M. Haeussler, S.W.B. Klaassen, and D.J. Rixen. Experimental twelve degree of freedom rubber isolator models for use in substructuring assemblies. *Journal of Sound and Vibration*, 474:115253, 2020.
- [5] Marco Lovera, Carlo Novara, Paulo Lopes dos Santos, and Daniel Rivera. Guest editorial special issue on applied lpv modeling and identification. *IEEE Transactions on Control Systems Technology*, 19(1):1–4, 2011.
- [6] Carlo Novara, Fredy Ruiz, and Mario Milanese. Direct identification of optimal sm-lpv filters and application to vehicle yaw rate estimation. *IEEE Transactions on Control Systems Technology*, 19(1):5–17, 2011.
- [7] Jan De Caigny, Juan F. Camino, and Jan Swevers. Interpolation-Based Modeling of MIMO LPV Systems. *IEEE Transactions on Control Systems Technology*, 19(1):46–63, 2011.

- [8] Jan De Caigny, Juan F. Camino, and Jan Swevers. Interpolating model identification for siso linear parameter-varying systems. *Mechanical Systems and Signal Processing*, 23(8):2395–2417, 2009.
- [9] Federico Felici, Jan-Willem van Wingerden, and Michel Verhaegen. Subspace identification of mimo lpv systems using a periodic scheduling sequence. *Automatica*, 43(10):1684–1697, 2007.
- [10] Jan De Caigny, Rik Pintelon, Juan F. Camino, and Jan Swevers. Interpolated Modeling of LPV Systems. *IEEE Transactions on Control Systems Technology*, 22(6):2232–2246, 2014.
- [11] Francesco Ferranti and Yves Rolain. A local identification method for linear parameter-varying systems based on interpolation of state-space matrices and least-squares approximation. *Mechanical Systems and Signal Processing*, 82:478–489, 2017.
- [12] Per Sjövall and Thomas Abrahamsson. Component system identification and state-space model synthesis. *Mechanical Systems and Signal Processing*, 21:2697–2714, 2007.
- [13] R.S.O. Dias, M. Martarelli, and P. Chiariotti. Lagrange Multiplier State-Space Substructuring. *Journal of Physics: Conference Series*, 2041(1):012016, 2021.
- [14] R.S.O. Dias, M. Martarelli, and P. Chiariotti. On the use of lagrange multiplier state-space substructuring in dynamic substructuring analysis. *Mechanical Systems and Signal Processing*, 180:109419, 2022.
- [15] R.S.O. Dias, M. Martarelli, and P. Chiariotti. Including connecting elements into the lagrange multiplier state-space substructuring formulation. *Journal of Sound and Vibration*, 546:117445, 2023.
- [16] R.S.O. Dias, M. Martarelli, and P. Chiariotti. In-situ component-based tpa for time-variant dynamic systems: A state-space formulation. In Matthew Allen, Walter D’Ambrogio, and Dan Roettgen, editors, *Dynamic Substructures, Volume 4*, pages 73–87, Cham, 2024. Springer Nature Switzerland.
- [17] M. Allen, D. Rixen, M.V. van der Seijs, P. Tiso, T. Abrahamsson, and R. Mayes. *Substructuring in Engineering Dynamics*. Springer International Publishing, 2020.
- [18] J.H. Yung. *Gain scheduling for geometrically nonlinear flexible space structures (PhD dissertation)*. Massachusetts Institute of Technology, Cambridge, MA, USA, 2002.
- [19] J. Brewer. Kronecker products and matrix calculus in system theory. *IEEE Transactions on Circuits and Systems*, 25(9):772–781, 1978.
- [20] Mahmoud El-Kafafy and Bart Peeters. A Robust Identification of Stable MIMO Modal State Space Models. In: *Dilworth, B.J., Marinone, T., Mains, M. (eds) Topics in Modal Analysis & Parameter Identification, Volume 8. Conference Proceedings of the Society for Experimental Mechanics Series. Springer, Cham*, pages 81–95, 2023.
- [21] Peter Avitabile. *Modal testing: a practitioner’s guide*. John Wiley & Sons, 2017.
- [22] Dao Gong, Yu Duan, Kang Wang, and Jinsong Zhou. Modelling rubber dynamic stiffness for numerical predictions of the effects of temperature and speed on the vibration of a railway vehicle car body. *Journal of Sound and Vibration*, 449:121–139, 2019.
- [23] J. Wojtowicki and S. Lecuru. Characterization and modelling of mounts for electric powertrains. In: *12th International Styrian Noise, Vibration Harshness Congress: The European Automotive Noise Conference*, pages 952–964, 2022.
- [24] Bart Peeters, Herman Van der Auweraer, Patrick Guillaume, and Jan Leuridan. The polymax frequency-domain method: a new standard for modal parameter estimation? *Schock and Vibration*, 11:395–409, 2004.

- [25] Mahmoud El-Kafafy, Bart Peeters, Patrick Guillaume, and Tim De Troyer. Constrained maximum likelihood modal parameter identification applied to structural dynamics. *Mechanical Systems and Signal Processing*, 72-73:567–589, 2016.
- [26] R.S.O. Dias, M. Martarelli, and P. Chiariotti. State-space domain virtual point transformation for state-space identification in dynamic substructuring. In: *Proceedings of ISMA 2022 - International Conference on Noise and Vibration Engineering and USD 2022 - International Conference on Uncertainty in Structural Dynamics*, 2022.
- [27] A. Liljerehn. *Machine Tool Dynamics – A Constrained State-space Substructuring Approach (Doctoral thesis)*. Chalmers University Technology, Göteborg, Sweden, 2016.
- [28] Steven Gillijns and Bart De Moor. Unbiased minimum-variance input and state estimation for linear discrete-time systems with direct feedthrough. *Automatica*, 43(5):934–937, 2007.
- [29] Accelerometer, icp[®], triaxial, model 356a32. <https://www.pcb.com/products?m=t1d356a32>. Accessed: 2023-05-15.